AD-A117 892 TEXAS UNIV AT AUSTIN DEPT OF CHEMISTRY F/6 7/4
PROPERTIES OF PT SUPPORTED ON OXIDES OF TITANIUM.(U)
JUN 82 B CHEN, J M WHITE N00014-75-C-0922
UNCLASSIFIED TR-23 NL

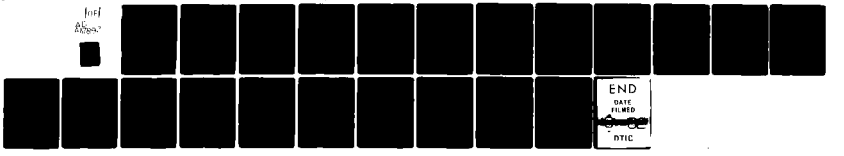

END
DATE FILMED
DTIC

(12)

OFFICE OF NAVAL RESEARCH

Contract N00014-75-C-0922

Task No. NR 056-578

TECHNICAL REPORT NO. 23

Properties of Pt Supported on Oxides of Titanium

by

Bor-Her Chen and J. M. White

Prepared for publication

in

Journal of Physical Chemistry

Department of Chemistry

University of Texas at Austin

Austin, Texas 78712

June 9, 1982

SECURITY CLASSIFICATION OF THIS PAGE (When Data Entered)

REPORT DOCUMENTATION PAGE		READ INSTRUCTIONS BEFORE COMPLETING FORM
1. REPORT NUMBER	2. GOVT ACCESSION NO. AD-A117692	3. RECIPIENT'S CATALOG NUMBER
4. TITLE (and Subtitle) Properties of Pt Supported on Oxides of Titanium		5. TYPE OF REPORT & PERIOD COVERED Technical Report 23 Jan. 1, 1982-Dec. 31, 1982
		6. PERFORMING ORG. REPORT NUMBER
7. AUTHOR(s) Bor-Her Chen and J. M. White		8. CONTRACT OR GRANT NUMBER(s) N00014-75-C-0922
9. PERFORMING ORGANIZATION NAME AND ADDRESS J. M. White Dept. of Chemistry, University of Texas Austin, TX 78712		10. PROGRAM ELEMENT, PROJECT, TASK AREA & WORK UNIT NUMBERS Project NR-056-578
11. CONTROLLING OFFICE NAME AND ADDRESS Department of the Navy Office of Naval Research Arlington, VA 22217		12. REPORT DATE 6-9-82
		13. NUMBER OF PAGES 33
14. MONITORING AGENCY NAME & ADDRESS(if different from Controlling Office)		15. SECURITY CLASS. (of this report)
		15a. DECLASSIFICATION/DOWNGRADING SCHEDULE
16. DISTRIBUTION STATEMENT (of this Report) Approved for public release: distribution unlimited		
17. DISTRIBUTION STATEMENT (of the abstract entered in Block 20, if different from Report)		
18. SUPPLEMENTARY NOTES Preprint; in press, Journal of Physical Chemistry		
19. KEY WORDS (Continue on reverse side if necessary and identify by block number)		

20. ABSTRACT (Continue on reverse side if necessary and identify by block number)

Platinum, supported on TiO_2, TiO and Ti_2O_3 in various forms, has been investigated using a variety of physical and chemical techniques. On H_2 pretreated TiO_2, on TiO and on Ti_2O_3 samples (all platinized), SMSI behavior, i.e. limited H_2 uptake, was noted. Very fast H-for-D exchange rates were observed for H_2D_2 mixtures on all these materials indicating that dissociative adsorption still occurs readily. Using XPS, SAES, TEM and STEM data we conclude that surface contamination, diffusion of Pt into the bulk oxide, formation of

DD FORM 1 JAN 73 1473 EDITION OF 1 NOV 65 IS OBSOLETE
S/N 0102-014-6601

SECURITY CLASSIFICATION OF THIS PAGE (When Data Entered)

Block 20. Continued.

surface mixed metal oxides and metal agglomeration are not significant contributors to the observed loss of H_2 uptake capacity. On the basis of qualitative bulk electrical conductivity data and XPS data, we suggest that the SMSI effect is best understood in terms of a bulk oxide reduction model. In this model, bulk conduction band electrons tunnel readily through a thin TiO_2 layer at the surface to reach Pt particles where they are trapped and furnish a negatively charged Pt particle with good capacity for dissociating H_2 but weak binding of atoms.

5-10-82
106
revised
J. Phys. Chem. (in press)
5/82.

Properties of Pt Supported on Oxides of Titanium[a]

Dor-Her Chen[b] and J. M. White[c]

Department of Chemistry

University of Texas

Austin, TX 78712

(a) Supported in part by the Office of Naval Research.

(b) Permanent address: Department of Chemistry, Tankang University, Tamsui, Taipei 251, Taiwan, R.O.C.

(c) Author to whom correspondence should be addressed.

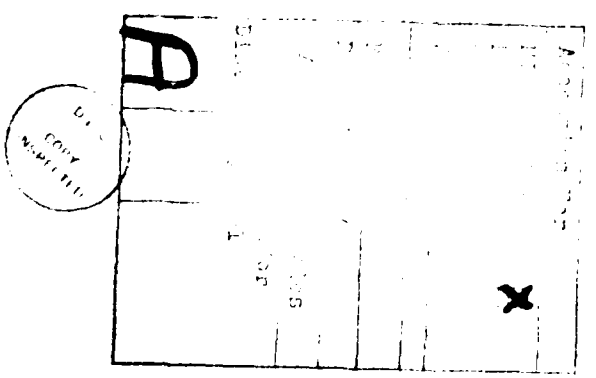

ABSTRACT

Platinum, supported on TiO_2, TiO and Ti_2O_3 in various forms, has been investigated using a variety of physical and chemical techniques. On H_2 pretreated TiO_2, on TiO and on Ti_2O_3 samples (all platinized), SMSI behaviour, i.e. limited H_2 uptake, was noted. Very fast H-for-D exchange rates were observed for H_2-D_2 mixtures on all these materials indicating that dissociative adsorption still occurs readily. Using XPS, SAE, TEM and STEM data we conclude that surface contamination, diffusion of Pt into the bulk oxide, formation of surface mixed metal oxides and metal agglomeration are not significant contributors to the observed loss of H_2 uptake capacity. On the basis of qualitative bulk electrical conductivity data and XPS data, we suggest that the SMSI effect is best understood in terms of a bulk oxide reduction model. In this model, bulk conduction band electrons tunnel readily through a thin TiO_2 layer at the surface to reach Pt particles where they are trapped and furnish a negatively charged Pt particle with good capacity for dissociating H_2 but weak binding of H atoms.

1. INTRODUCTION

The use of transition metal/titania systems has recently received considerable attention in two areas--photoassisted reactions at the gas-solid or liquid-solid interface and strong metal support(SMSI) interaction phenomena. As part of our continuing research on photoassisted reactions[1], we have undertaken work to characterize the substrates we have been using in an effort to understand the role of SMSI effects. This paper reports part of that work.

The SMSI effect, which is characterized by a strongly reduced uptake of hydrogen and carbon monoxide on suppported transition metals,[2] has recently drawn intense attention because of promising potential in controlling the activity and selectivity of catalysts.[3-5] The alteration of catalytic properties through interactions with the substrate is a very interesting approach to the development of promising catalytic materials for both conventional and photoassisted heterogeneous reactions.

In this paper we report studies of platinized oxides of titanium, including various forms of TiO_2, TiO and Ti_2O_3. A variety of bulk and surface measurements are reported which provide some clarification of the nature of the interactions between platinum and the oxide supports.

2. EXPERIMENTAL

The TiO_2 (reagent grade anatase, < 125 μm diameter particles) was obtained from MCB. Ti_2O_3 and TiO powders (99+%, optical grade) were obtained from Alpha Products. Chloroplatinic acid, H_2PtCl_6, was prepared by dissolving Pt foil (99.99%) in aqua regia. Research grade H_2 and D_2 (98%) were obtained from Linde. Both were purified by passage through a 5A molecular sieve trap immersed in liquid nitrogen.

Two types of anatase were used as support materials: (1) as received from the manufacturer and (2) an H_2 pretreated sample prepared by reducing the above anatase in flowing H_2 (30 ml/min) at 875°C for 6 hr and denoted as $TiO_2(H_2$ pre).

One set of 2 wt.% Pt catalysts was prepared by impregnating all the support powders with 0.1 N H_2PtCl_6 solution. A second set was prepared by a photodecomposition method.[6] An oxidized form of the $TiO_2(H_2$ pre) catalyst was prepared exposing the reduced material to 550 Torr of O_2 at 500°C for 17 hr.

Surface areas (N_2 adsorption at 77 K) and H_2 chemisorption measurements were carried out in a standard static volumetric apparatus. For the H_2 uptake measurements, each sample was: (1) degassed for one hr at 200°C under dynamic vacuum of 10^{-6} Torr, (2) reduced for 2 hr. with 550 Torr H_2 at 200°C, (3) degassed again at 200°C for one hr., (4) cooled to room temperature under dynamic vacuum and (5) exposed to H_2 for the uptake measurement. For one sample, the temperature in steps (1), (2) and (3) was raised to 400°C with no detectable effect on the H_2 uptake isotherm. Therefore, 200°C was used routinely.

The H_2-D_2 isotope exchange studies were carried out in an evacuable, circulation-pumped system (230 ml volume) which was connected to a mass

spectrometer for reaction product analysis. The catalyst was spread uniformly on one face of a quartz reaction vessel (used in related photoassisted reactions) which was part of the circulation loop. In each exchange experiment, 1.1 Torr of an equimolar H_2-D_2 mixture was dosed into the reactor loop from a connected storage vessel.

Qualitative electrical conductivity measurements were made by pressing the powdered catalyst in a pellet die under 10,000 psi for 5 min. The electrical resistance of the pellet was determined by measuring the current through the pellet-die assembly when a fixed voltage was applied. The thickness and the cross-section of the pellet were measured so that the specific electrical conductivity could be calculated. These measurements have been used only for qualitative guidance.

The X-ray powder diffraction patterns were obtained with a conventional diffractometer (Philips). The SEM studies utilized a model JSM-35C, JEOL system and the TEM and STEM measurements were done on a JEOL 100B system. For the TEM study, samples were dispersed on carbon-coated grids using a sonicated mixture of catalyst and chloroform.

X-ray, and electron spectra (XPS) and scanning Auger spectra (SAES) were taken with two Physical Electronics Industries (PHI) instruments. In the XPS studies, some sample pellets were pretreated in a reaction chamber attached to the spectrometer vacuum chamber. Conditions could be chosen to simulate those used in the H_2 uptake experiments. For these experiments, a Mo or Ta mask was used to hold the sample against a button heater. In cases where no simple heating was necessary, the powders were pressed into In foil. The relative atomic compositions of the surface layers studied by XPS were calculated from the relative peak areas adjusted for atomic sensitivities taken from the PHI handbook. The SAES measurements were made in a background pressure of 3×10^{-9} Torr using a 3 KeV electron beam.

Atomic composition ratios were calculated from peak-to-peak height ratios and tabulated atomic sensitivity factors.

3. Results

3.1 H_2 Adsorption Isotherms.

Table 1 lists a series of materials used in this work. Included are various bulk oxides of titanium, including hydrogen treated and oxidized forms, some of which were platinized. As noted above, two platinization techniques were used, impregnation (imp) and photoreduction (photo). As a standard for comparison and for checking the performance of our apparatus, a commercial Pt/Al_2O_3 sample was also included.

All the hydrogen adsorption isotherms were recorded at room temperature. Representative data is given in Figs. 1-2 and the extent of the uptake at low pressures (< 1 Torr) is tabulated in Table 1. Upon exposure to H_2, curve (a) of Fig. 1 shows a strong chemisorption step while curve (b) does not. These two samples are typical of the kind of results which we observe; deposition of Pt on prereduced TiO_2 by either the photoreduction method or the standard impregnation procedure gives a sample which will not chemisorb significant amounts of hydrogen unless it is first oxidized at high temperatures. Curve (b) is data for a platinized sample prepared by the photoreduction method and, just before the H_2 uptake experiments, was exposed to H_2 at [illegible]K and then evacuated at the same temperature. Curve (a) is for this same sample but after oxidation at [illegible]K. The extrapolated amount of chemisorbed hydrogen is [illegible] μmole gm^{-1} of catalyst and corresponds to a H/Pt ratio of [illegible]. This is to be compared with a calculated H/Pt ratio of [illegible] based on an average Pt crystallite size of [illegible]Å (STEM measurement described below) and the assumption of hemispherical particles. For reduced catalysts, STEM measurements indicate a slightly smaller particle size.

It is important to note here that strong H_2 chemisorption is also found on Pt/TiO_2 using titania that is neither prereduced nor oxidized before the

H_2 chemisorption experiment. This demonstrates that the strong chemisorption noted in the previous paragraph is not the result of cleaning off impurities during oxidation.

Curves (c) and (d) of Fig. 1 are for platinized (by impregnation) samples of Ti_2O_3 and TiO respectively. They show no chemisorption step and follow the same uptake trends with increasing H_2 pressure as the other samples.

The absence of a chemisorption step in the hydrogen uptake is a characteristic feature of SMSI[2]. However, it is significant to note here that XPS indicates that the surfaces of all of these materials are oxidized to TiO_2. Since the support materials are all exposed to air before platinization and since the reduced surfaces are relatively easily oxidized as shown by ESR[7], XPS of powders[2] and XPS of thin films[9], it is not surprising that the surfaces were all found by XPS to be TiO_2. The implication is that SMSI properties are present when the subsurface (bulk) is reduced even when the topmost layers are fully oxidized. This will be discussed further below.

Figure 2 shows, as indicated, the H_2 uptake for these oxides in the absence of Pt. As expected there is no chemisorption, only the slowly rising uptake typical of physisorption on oxides and very much like what is seen in Fig. 1 for the platinized forms. The only difference is that the slow uptake is somewhat more extensive in the presence of Pt. This is supported by infrared transmission measurements to be reported elsewhere[10] which show that surface OH is formed upon exposure of platinized titania to H_2. We take this to mean that Pt promotes dissociative adsorption of hydrogen even when it is in a state that does not allow a sizeable surface concentration to develop and that migration from Pt to the oxides of titanium occurs, i.e. spillover.

Returning to a consideration of curves (a) and (b) of Fig. 1, we note

that the uptake of hydrogen at 440 Torr corresponds roughly to a coverage of one monolayer over the oxide support based on a BET surface area of 10 m^2 gm^{-1} and a one monolayer concentration of 10^{19} m^{-2}. The slowly rising isotherms shown in Figs. 1 and 2 are reversible. After evacuating the system overnight at room temperature and 10^{-6} Torr, refilling with hydrogen gave the same slowly rising uptake curve. The strongly chemisorbed hydrogen (10 μmole/gm in Fig. 1a) could be completely removed by heating the catalyst to 400°C for one hour. A significant fraction, but certainly not all, of it was desorbed by heating at 300°C for one hour and no desorption was noted during one hour heating at either 100 or 200°C.

The inset of Fig.2 shows the results of a control experiment with a commercial Pt/Al_2O_3 catalyst (Matthey) having, according to the manufacturer,[11] a dispersion of 0.45. Our results, extrapolated to zero pressure, give 0.37 which we regard as acceptable agreement.

3.2 Catalyst characterization by spectroscopic methods.

X-ray diffraction data are given in Table 1. Prior to the H_2 treatment the X-ray powder diffraction pattern was dominated by anatase peaks at 2θ values of 25.26°, 36.96°, 37.76°, 38.56°, and 48.10° and no rutile peaks were found. After reduction, rutile peaks appeared at 27.44°, 36.12°, 39.2°, 41.16° and 44.04°. Even though these samples were dominated by rutile, we note that samples dominated either by rutile or anatase show strong hydrogen chemisorption provided the substrate is oxidized. For example, Pt/TiO_2 formed from unreduced TiO_2 is dominated by anatase and shows the same hydrogen uptake as a heavily reduced Pt/TiO_2 that is reoxidized (dominated by rutile). Additional peaks, which we attribute to Ti_9O_{17} appear in the spectra for samples 2 and 4, i.e. at 26.64°, 28.18°, 35.16° and 35.86° (not resolved). Upon oxidation, these Ti_9O_{17} peaks disappear.

Small peaks due to Pt crystallites were observable for all of the platinized samples. Judging from the intensity and apparent widths of these

[illegible], keeping in mind that the loading is 2 wt.% Pt in each case, we [illegible] that some sintering may occur in oxidizing the Pt/Ti_2O_3. The Pt peaks in spectra 9 and 11 indicate dispersions somewhat higher than for the samples containing TiO_2.

It is important to note that the light blue dot and the extra X-ray peaks due to bulk Ti_9O_{17} which appear when TiO_2 is treated with H_2, are very stable in room temperature air and upon platinization by either impregnation or photodeposition. Oxide ion (550 Torr O_2, 200°C, 12 hr.) not only removes the Ti_9O_{17} X-ray peaks but also restores the blue color; in the presence of Pt the purple becomes white while in the presence of Pt it becomes golden brown. The former color is characteristic of fully oxidized Ti, i.e. TiO_2, and the latter is characteristic of oxidized Pt.

TEM measurements on the Pt/TiO_2 (H_2 pre) samples prepared by the photodeposition and impregnation methods, indicate a broad range of Pt crystallite sizes -- 5 to several hundred Å. TEM measurements show similar results. Particle identification as Pt was made by energy dispersive X-ray analysis. These together with X-ray data show that the particle size distribution is broad. The average particle size is estimated as 200 Å and the Pt particles made by the photodeposition method is, at most, only slightly higher than with the impregnation method.

TEM measurements indicate that oxidizing the Pt/Ti_2O_3, for example, sample (b) of Fig. 1, is accompanied by very little change in the Pt particle size distribution. TEM measurements on the dark sample were inconclusive because the contrast between Pt and the oxide was very poor.

X-ray photoelectron spectra (XPS) were taken to identify the surface composition and chemical environment. Six samples were investigated: (1) TiO_2(anatase), (2) Pt/TiO_2(H_2 pre), (3) oxidized Pt/TiO_2 (H_2 pre), (4) Pt/Ti_2O_3, (5) Pt/TiO and (6) Pt/Al_2O_3. Some of these were examined after reduction in H_2 for 2 hr at either 200 or 500°C in the photoelectron

spectrometer ionization chamber. AES was used to examine the Pt/Ti_xO_y and Pt/TiO samples.

The results, summarized in Table 2 indicate a relatively large amount of surface carbon is present in every case although the C/Ti ratio is somewhat smaller for the Ti_xO_y and TiO-based samples. This surface carbon, which we were unable to reduce significantly by pretreatment in the reaction chamber, did not interfere with hydrogen chemisorption on the Pt/Al_2O_3 and oxidized Pt/TiO_2 (H_2 pre) samples. Moreover, samples using TiO and Ti_xO_y, which have smaller relative amounts of surface carbon (based on SAES results and probably due to overnight pumping before taking spectra), show very little chemisorption of hydrogen at low pressure. This evidence is consistent with notion that the presence of surface carbon is not correlated with H_2 chemisorption. We take this to mean that most of the carbon is on the oxide support.

Other possible poisons, including sulfur, phosphorus and chlorine, may also be ruled out as controlling the nature of the H_2 adsorption in these experiments. This is supported by the XPS data for which both the oxidized and not oxidized Pt/TiO_2/H_2 pre) samples show none of these species but their H_2 chemisorption properties are very different.

The binding energies shown in Table 2 are all referenced to the C(1s) signal which was set at 284.6 eV after initial calibration using the Au($4f_{7/2}$) peak at 83.8 eV. The carbon 1s binding energy was first determined as 284.6 eV using a pellet of titania coated with carbon-containing material as a result of pressing it with paraffin paper on the die faces. In the absence of this carbon XPS gave a much lower C(1s) intensity at the same BE.

The Ti($2p_{3/2}$) BE's listed in Table 2 all lie within a 1 eV region and the shifts do not correlate with SMSI behavior. For example, the BE of the surface Ti($2p_{3/2}$) is 458.9 eV for both Pt/Ti_2O_3 (catalyst F) which shows the

SMSI property and for oxidized Pt/TiO_2 (H_2 pre) (catalyst B) which does not show the SMSI property. The bulk of all the TiO and Ti_xO_y samples is definitely dominated by Ti^{2+} and Ti^{3+} respectively (XRD data) while the surface is oxidized to Ti^{4+}. Sayers and Armstrong [12] reported that the binding energy shift, $\Delta BE = (Ti(2p)-Ti(2p_{3/2})$, depends on the oxidation state of Ti but is nearly independent of the physical form of the titanium oxides. They find for TiO_2 samples, ΔBE is 71.5 ± 0.4 eV, while for Ti_2O_3 and TiO samples, the values are 73.4 ± 0.4 eV and 74.0 ± 0.2 eV, respectively. Our results give ΔBE = 71.3 ± 0.2 eV for platinized catalysts with and without SMSI property (B to H, Table 2) indicating that there are no detectable Ti^{+2} or Ti^{+3} species present on the surfaces of these Pt catalysts showing the SMSI property. We conclude that there is no relation between the SMSI effect and the oxidation state of the detectable surface Ti ions.

High resolution XPS spectra (25 eV pass energy, with an analyzer resolution of ΔE = 0.4 eV) of catalysts with (C, E, F and H) and without (B) the SMSI property are shown in Fig. 3. The peak positions and half-widths are given in Table 2. Reduction does not lead to a significant increase in FWHM of the Ti($2p_{3/2}$) peak; rather a decrease from 1.83 to 1.44 eV is found as indicated in Table 2, samples B and C. Thus, there is no evidence for mixed Ti states upon reduction. We attribute the linewidth variations to changes in surface heterogeneity.

Figure 4 shows XPS for the Pt(4f) region of materials with (E, F and H) and without (B) SMSI behavior. The BE's range from 70.5 to 71.1 eV with no correlation with the SMSI property. Catalyst F, with SMSI, has a Pt($4f_{7/2}$) BE of 70.9 eV while catalyst B, non-SMSI, has a peak at 71.1 eV.

The surface atomic Pt/Ti ratios calculated from the XPS peak areas are also listed in Table 2. The results indicate that the SMSI property is not due to diffusion of Pt into the subsurface during reduction. Materials with SMSI behavior (C, E, F and H) show Pt/Ti between 0.06 and 0.36 clearly

indicating that a significant amount of Pt is present on the surface. The results from SAES also confirm this point although their values (Table 2, Catalysts I and J) are somewhat different from the XPS results. Comparing B and C in Table 2 shows that the Pt/Ti ratio does decrease from 0.11 to 0.07 upon reduction at 500°C but this loss cannot account for the total depression of measurable H_2 chemisorption that is observed. In fact, the observed loss is almost within the limits of our ability to detect a significant change in the surface Pt concentration. With reduction, changes in surface morphology (roughness) and changes in surface contamination can account for the observed Pt/Ti variations.

3.3 H_2-D_2 Isotope Exchange.

The results of exposing the catalyst to an equimolar mixture of hydrogen and deuterium are summarized in Table 3 using a concentration function in the form of the equilibrium constant. As thermodynamic equilibrium is approached, the value of this function will increase. The values were calculated from mass spectrometric peak heights assuming no difference in sensitivity among the isotopic forms of molecular hydrogen.

The results are very informative in the sense that none of the Pt-free substrates shows much activity for the exchange. On the other hand, all of the platinized catalysts exhibit very rapid exchange and the rate of approach to equilibrium is at least as fast for the Pt/TiO_2(H_2 pre, photo) as it is for the unreduced Pt/TiO_2. Even though the former shows no chemisorption, while the latter does, both readily catalyze the H-for-D exchange reaction. We take this as evidence for the ready dissociation of hydrogen by Pt on both samples with a much more rapid desorption on the former. The same kind of process is proposed to account for the relatively rapid isotope exchange on both Pt/TiO and Pt/Ti_2O_3 neither of which shows any measurable chemisorption of hydrogen at room temperature. The observation of rapid isotope exchange also supports the conclusion drawn in section 3.2 that the relatively large amounts of surface carbon detected by XPS are located primarily on the oxide support and do not interfere with hydrogen adsorption at Pt sites.

It is important to consider the possibility that the exchange reaction is catalyzed by a small number of Pt sites in contact with TiO_2, i.e. only a small fraction of the total amount of Pt is active for the dissociation of H_2. If this is the case, then the observed exchange rate per site is extremely fast and exceeds the rate on Pt which shows strong chemisorption of hydrogen. Although we do not favor this model, it is a possibility if

the interaction between Pt and the underlying TiO_2 activates certain of the Pt atoms.

3.4 Electrical Conductivity Measurements.

The results for electrical conductivity and surface area are summarized in Table 3. The starting material(A) has a specific electrical conductivity of less than $2 \times 10^{-11} ohm^{-1}cm^{-1}$. This increases by more than two orders of magnitude after heating in hydrogen for 17 hr at 875°C, sample C. Sample B is the same material as C except it was carried through the photoplatinization procedure without using any H_2PtCl_6 in the solution. Platinization of C gives a sample D which has lower specific electrical conductivity, 4.7×10^{-10} ohm^{-1} cm^{-1}. Our reproducibility is about ± 20%, compare D and E, so this change is significant. Comparing the pairs F, G and H, I, indicates that platinization reduces the specific electrical conductivity of TiO and Ti_2O_3 samples by about one order of magnitude. We attribute these decreases to electrons being tied up at surface Pt particles, or species attached to the Pt, thereby decreasing the conduction electron density. With these measurements alone, we cannot rule out the possibility that conductivity changes are the result of variations in either particle-particle contact resistance or charge localization at species chemisorbed on Pt. However, taken with the other data presented here, an internally consistent model involves localization of charge on Pt particles when the underlying oxide is reduced.

4. DISCUSSION

As noted above, the H_2 uptake data, the XRD patterns, the isotope exchange rates, the XPS and SAES data, the electron microscopy results and the electrical conductivity data are all consistent with a model in which the SMSI behavior is dependent upon the ability of the support to donate electrons to the Pt particles. We discuss here in more detail our views about the requirement of bulk reduction in order to observe SMSI and why catalysts which do not accumulate significant coverages of dissociated hydrogen nevertheless exchange hydrogen isotopes very rapidly.

The inability to detect measurable amounts of Ti^{2+} or Ti^{3+} species by XPS on TiO, Ti_2O_3 or $TiO_2(H_2$ pre) surfaces exposed to air at room temperature (Section 3.2), all of which show SMSI behavior, suggests that electron transfer occurs from reduced subsurface regions to Pt crystallites through a thin barrier layer of TiO_2. Without significant bulk conductivity, it is difficult to explain the observed effects in terms of $Pt-Ti^{n+}$ metal-metal bonds ($n < 4$) because the surface is oxidized before the Pt is deposited. Consequently, differences in the subsurface (bulk) regions of these materials may play a key role. This bulk conductivity model correlates the SMSI and electrical conductivity data quite well, particularly when we keep in mind the XRD and XPS results. The electrical conductivity decreases in $TiO_2(H_2$ pre), Ti_2O_3 and TiO when platinized while it increases in TiO_2. The SMSI effect follows the same pattern.

Using ESR to detect Ti^{3+}, Huizinga and Prins [13] studied the surface reduction of Pt/TiO_2 at 300°C and 500°C finding reversibility at the lower but not the higher temperature. They attribute this to the formation of microcrystals of Ti_4O_7 formed at the higher temperature as the result of dehydration. Since SMSI behavior is observed after 500°C, but not 300°C, reduction [2], we infer that local low temperature surface reduction of

titania by spillover of H to form Ti^{3+} and OH^- is not the source of the SMSI behavior. The irreversible formation of Ti_4O_7 or Ti_9O_{17} microcrystals (i.e. bulk reduction) at the higher temperatures is consistent with the ESR data and the observed SMSI character. Huizinga and Prins [13] suggest that the appearance of these crystallites near the surface leads to morphological and electronic structure changes in the Pt particles as proposed by others [2,14]. In related work, Apple et al. [15] report that strong H_2 chemisorption is found by NMR for Ru/TiO_2 catalysts with both large and small ESR signals due to Ti^{3+}. Since, for their conditions, surface reduction would dominate, we infer that the presence of significant surface Ti^{3+} concentrations does not guarantee SMSI behavior. Our results are also consistent with a model requiring more than surface Ti^{3+}. Indeed, recent ESR work in our laboratory[16] shows that the SMSI property is correlated with the presence of bulk Ti^{3+} signals that are not subject to reversible formation/removal upon exposure/evacuation of H_2 at around room temperature.

The isotope exchange and H_2 uptake data suggest that the dissociative reaction probabilities are about the same on SMSI and non-SMSI catalysts. The heats of adsorption are, however, significantly different, the SMSI catalysts having lower values. A more quantitative description could be developed using a Langmuir isotherm formulation but our data does not permit a quantitative evaluation. Figure 5a shows schematically how H_2 interacts with a Pt catalyst which does not exhibit SMSI. There is a small activation energy, E_{a1}, for dissociative adsorption and a rather large activation energy, E_{d1}, for desorption. The high value of the latter favors a high surface coverage at equilibrium and temperatures near 25°C. Rapid isotope exchange in the H_2-D_2 equilibration is the result of high surface coverages compensating partially for the relatively high activation energy of desorption. In the SMSI case, Fig. 5b, the activation energy for dissociative adsorption, E_{a2}, is assumed to be about equal to E_{a1} but the heat of adsorption, E_{d2}, is taken to be much smaller than E_{d1}. Here, low hydrogen coverages at equilibrium are expected, as observed. The unfavorable effect of low hydrogen coverage on the isotope exchange rate is compensated by the low energy required for desorption. In fact, we should not be surprised to find exchange rates proceeding more rapidly on the SMSI materials; the lifetime of a hydrogen atom on the surface is shorter but the dissociative adsorption probability at zero coverage is about the same with the model of Fig. 9. Consequently, the steady state rate of adsorption, and the rate of exchange, will be more rapid for the SMSI case.

Shorter residence times for H atoms on SMSI surfaces have been proposed by Tauster et al.[17] to account for the higher activity and selectivity of Ni/TiO_2 as compared with Ni/SiO_2 or Ni/Al_2O_3, for Fischer-Tropsch synthesis. The model of Fig. 5 can account for these differences. The shorter lifetime is beneficial to higher activity so long as it is long enough to allow the reaction of interest to compete effectively with other reactions.

In agreement with Baker et al.[14], who used TEM, our results using XRD and TEM indicate that SMSI is not the result of agglomeration of Pt during various treatments. Neither surface impurity poisons nor diffusion of Pt into subsurface regions are significant contributors to the SMSI effect according to our XPS, H_2 uptake and H_2-D_2 exchange results.

Tauster et al.[17] have suggested that the degree of SMSI effect reached depends upon the ease with which the metal oxide is reduced to provide electron rich cations at the surface which form metal-metal bonds with deposited Group VIII metals like Pt. Our results are consistent, in part, with this model. However, we favor a model in which attention is focussed on the reduction of the bulk which supplies electrons to the adsorbed Pt and lowers their ability to bind atomic hydrogen. A slight change in the language, will bring the two models into agreement. In

selecting materials for an SMSI effect, we propose choosing a support with relatively high electrical conductivity and a work function lower than the deposited metal. To achieve n-type electrical conductivity in typical metal oxides, reduction to remove lattice oxygen must be carried out. The more readily this occurs, the stronger the SMSI effect. By reduction, not only is the conductivity changed, the work function also decreases as the Fermi level moves toward the bottom of the conduction band. For charge transfer from support to Pt upon platinization, the work function of the support must be smaller than that of the metal, i.e. the highest occupied levels of the support lie above the highest occupied levels of the Pt before contacting the two. Materials with low conductivity will not show SMSI unless dopants supplying charge carriers to the conduction band are introduced.

Although p-type semiconductors can be included in this description, electron transfer to Pt from the support will require a "hopping" scheme from one acceptor site to another. Consequently, relatively high doping, to bring these sites close enough for orbital overlap, is required. For n-type material, the conduction band is utilized, so all one needs is thermal excitation into the conduction band and tunneling through the contact barrier at the support/metal interface, i.e. at the TiO_2/Pt junction.

Supporting evidence based on electrical conductivity and type of charge carrier is given in Table 4. We agree completely with Tauster et al.[17] in considering the oxides which show SMSI; however, our description is somewhat broader and includes materials which are not easily reduced. For example, SiC is not in the oxide category and is not readily reduced.[18] In a separate study,[19] we have found SMSI behavior for Pt/SiC and an increased H_2-D_2 exchange rate upon platinization. This is consistent with our model and suggests that metal-metal bond formation is not a necessary condition for observing SMSI behavior.

Other H_2 uptake studies[20] also support the importance of the bulk

electrical conductivity and Fermi level position in SMSI. For example, no SMSI property is observed for the Pt/TiO_2 system if the titania is pretreated in flowing H_2 for 6 hr at 700°C and then platinized. As in the work reported here, we expect the surface to reoxidize during platinization and/or exposure to air. The absence of SMSI then suggests that the reduction process did not increase the bulk conductivity sufficiently and/or did not raise the Fermi level of the titania to a value high enough to permit charge transfer. Note that the work functions of undoped TiO_2 and Pt are 6.2 eV[21] and 5.7 eV[22], respectively.

We have also observed electron transfer from Pt to rutile by measuring the electrical properties(I, V, R and C) of a thin film of Pt deposited on single crystal rutile, pretreated in flowing H_2 for 1 hr at 500°C.[19]

The bulk effect charge transfer model suggested here is not new. Baddour and Deibert[23] proposed a similar model in 1966 to explain the promotion of Ni supported on Ge in the catalysis of formic acid decomposition. In another important contribution, Solymosi[24] has reviewed the catalytic importance of the electrical properties of supports. The implication of the bulk conductivity model for electron transfer is that as the metal crystallite or cluster size becomes smaller, the surface charge density will increase. This may account for the different catalytic behavior and the observed resistance to sintering for smaller particles.[25] Our model emphasizes the importance of electron transfer from the bulk of the support to the metal as the key for SMSI behavior. Electron transfer through interfacial metal-metal bonds or through tunneling, as described above, can result in SMSI effects. The negatively charged metal particles will tend to increase their surface areas to reduce their surface charge densities. The expected morphological changes have been observed by Baker, et al.[14] who found a tendency towards flatter pill-box Pt structures when Pt/TiO_2 was reduced at elevated temperatures.

Prior to reduction or after oxidation, the Pt particles had hemispherical shapes. We have found similar morpnology differences;[26] Pt/TiO_2 shows hemispherical Pt particles, Pt/TiO_2 (H_2 pre) shows polyhedral particles, and Pt/TiO shows raft-like particles.

One SMSI support which appears to fall completely outside the proposed selection rule is MnO; the reason is not clear, but it is worth noting that nonstoichiometric MnO is a semiconductor[27] while, in stiochiometric form it is an insulator.[17,28] Further study is required to clear up this question.

Speculation about the formation of mixed metal oxides in SMSI systems is not warranted here but it does deserve additional study. However, we note that the formation of mixed metal oxides typically requires an oxidizing environment in excess of 500°C. In order to avoid their formation and the possibility of significant impurity and/or diffusion of metal catalyst into the bulk of the support[29,30], our catalysts never encounter a temperature higher than 500°C, during or after platinization, so such mixed metal oxide effects are not likely to contribute significantly.

ACKNOWLEDGMENTS

The authors would like to express their hearty thanks to Dr. Marvin Deviney and Dr. Paul Buccemi for their kindness in taking most of the TEM and STEM micrographs for us. Thanks are also extended to Miss L. J. Fu for her assistance in running the SAES and Mr. Shiu-Min Fang for his assistance in making electrical conductivity measurements.

REFERENCES

1. a. S. Sato and J. M. White, J. Phys. Chem., 85(1981)592.
   b. S. Sato and J. M. White, J. Catalysis,
2. S. J. Tauster, S. C. Fung, R. L. Garten, J. Am. Chem. Soc., 100(1978)170.
3. a. M. A. Vannice and R. L. Garten, J. Catal., 56(1979)236.
   b. M. A. Vannice, S. H. Moon, C. C. Twu, Am. Chem. Soc., Div. Pet. Chem. preprints, 25(1980)303.
4. M. A. Vannice, J. Catal., 50(1977)228.
5. M. A. Vannice, S. H. Moon, S. Y. Wang, paper presented at American Chemical Society National Meeting, Houston, March 1980.
6. B. Kraeutler and A. J. Bard, J. Am. Chem. Soc., 100(1978)1694.
7. P. C. Gravelle, F. Juillet, P. Meriadeau and S. J. Teichner, Disc. Faraday Soc., 52(1971)140.
8. Powder pellets of TiO and Ti_2O_3 have been examined in our laboratory by John Schreifels and Bor-Her Chen.
9. John Schreifels, R. L. Hance, D. N. Belton, Bor-Her Chen and J. M. White, in preparation.
10. Katsumi Tanaka and J. M. White, J. Phys. Chem.(to be submitted).
11. Technical Service Department, Matheson Coleman & Bell Company, Cincinnati, Ohio.
12. C. N. Sayers and N. R. Armstrong, Surface Sci. 77(1980)301.
13. T. Huizinga and R. Prins, J. Phys. Chem. 85(1981)2156.
14. R. T. K. Baker, E. B. Prestridge and R. L. Garten, J. Catal., 59(1979)293.
15. T. M. Apple, P. Gajardo and C. Dybowski, J. Catal. 68(1981)103.
16. B.-H. Chen and J. M. White, unpublished data.
17. S. J. Tauster, S. C. Fung, R. T. K. Baker, J. A. Horsley, Science,

211(1981)1121.

18. E. A. Gulbranson and S. A. Jansson, Proc. Int. Congr. Met. Corros., 5th(1979)293.
19. Bor-Her Chen and J. M. White (in preparation).
20. S.-M. Fang, B.-H. Chen and J. M. White, J. Phys. Chem. (in press).
21. V. S. Fomenko, "Emission Properties of Elements and Chemical Compounds", Handbook (in Russian) Izd. Akad. Nauk Ukr. SSR (1965).
22. J. E. Demuth, Chem. Phys. Letters, 45(1977)12.
23. R. F. Baddour and M. C. Reibert, J. Phys. Chem., 70(1966)2173.
24. F. Solymosi, Catal. Rev., 1(1967)233.
25. R. T. K. Baker, E. B. Prestridge and R. L. Garten, J. Catal., 56(1979)390.
26. B.-H. Chen, J. M. White, M. L. Devinney and L. R. Brostrom, (to be submitted).
27. M. LeBlanc and H. Sachse, Z. Physik, 32(1931)887.
28. C. N. R. Rao and G. V. Subba Rao, Phys. Stat. Sol.(A) 1(1970)597.
29. C. C. Kuo, S. C. Tsai, M. K. Bahl and Y. W. Chung, Surface Sci., 95(1980)1.
30. B. J. Tatarchuk and J. A. Dumesic, J. Catal. 70(1981)308.
31. G. V. Samsonov, The Oxide Handbook, Plenum(New York, 1973).

Table 1. Summary of the Properties of Representative Samples.

Sample	H_2 uptake (μmole/gm)	Dispersion	H_2/O_2 Exchange	X-ray Powder Data	Average Pt Particle Size
1. TiO_2	0	--(a)	inactive	Ana(b)	----(c)
2. TiO_2(H_2 pre)	0	--	inactive	Ana, Rut, Ti_9O_{17}	----
3. Pt/TiO_2(imp)	10	0.20	active	Pt, Ana, Rut	----
4. Pt/TiO_2(H_2 pre, imp)	0	--	active	Pt, Ana, Rut, Ti_9O_{17}	100 A
5. Oxidized Pt/TiO_2 (H_2 pre, imp)	10	0.20	active	Pt, Ana, Rut	----
6. Pt/TiO_2(H_2 pre, photo)	0	--	active		100 A
7. Oxidized Pt/TiO_2 (H_2 pre, photo)	10	0.20	active	Pt, Ana, Rut	>100 A
8. Ti_2O_3	0	--	inactive	Ti_2O_3	----
9. Pt/Ti_2O_3(imp)	0	--	active	Pt, Ti_2O_3	----
10. TiO	0	--	inactive	TiO	----
11. Pt/TiO(imp)	0	--	inactive	Pt, TiO	----
12. 5 wt.% Pt/Al_2O_3	100	0.37	active	Pt/γ-Al_2O_3	----

Notes: a. (--) in the dispersion column indicates that this parameter can not be determined from hydrogen adsorption.

b. Ana = anatase, Rut = rutile, pre = prereduction, imp = impregnation

c. (----) in Pt particle size column indicates that this parameter was not determined.

Table 3. Surface Area, Electrical Conductivity and Isotope Exchange Data

No	Sample	Surface Area (m^2)	Specific Electrical Conductivity ($ohm^{-1}cm^{-1}$)	$(HD)^2/(H_2)(D_2)$ 25 sec	60 sec	300 sec	Temperature
A	TiO_2 0.35 gm	4.55	$<2.0 \times 10^{-11}$	10^{-3} 0.00 0.00	0.006 0.00 0.00	0.017 0.00 0.00	200°C 100°C 25°C
B	TiO_2(a*)		3.7×10^{-9}				
C	TiO_2(a) 0.35 gm	3.85	2.4×10^{-9}	2.8×10^{-3} 0.00 0.00	0.12 0.00 0.00	0.21 0.00 0.00	200°C 100°C 25°C
D	Pt/TiO_2(a) 0.35 gm SMSI	3.85	4.7×10^{-10}	1.20 ± 0.02 1.05 ± 0.05 1.01 ± 0.01	2.8 ± 0.2 2.51 ± 0.03 2.30 ± 0.10	3.31 ± 0.01 3.20 ± 0.02 3.07 ± 0.05	200°C 100°C 25°C
E	Pt/TiO_2 0.35 gm	3.85	5.0×10^{-10}	1.18 ± 0.02 0.82 ± 0.02 0.71 ± 0.01	2.4 ± 0.2 2.0 ± 0.1 1.82 ± 0.01	3.1 ±0.1 2.97 ± 0.01 2.72 ± 0.01	200°C 100°C 25°C
F	TiO 0.11 gm	3.85	1.2×10^{-1}	10^{-4} 0.00 0.00	5.4×10^{-4} 0.00 0.00	1.1×10^{-2} 0.00 0.00	200°C 100°C 25°C
G	Pt/TiO 0.11 gm	3.85	3.4×10^{-3}	1.3 1.1 ± 0.01 0.9 ± 0.1	2.82 ± 0.04 2.61 ± 0.03 2.22 ± 0.03	3.6 ± 0.1 3.49 ± 0.02 3.45 ± 0.02	200°C 100°C 25°C
H	Ti_2O_3 0.253 gm		6.1×10^{-3}		Not Done Not Done 0.00	0.00	200°C 100°C 25°C
I	Pt/Ti_2O_3 0.25 gm SMSI		6.2×10^{-4}	0.71 ± 0.09	Not Done Not Done 2.33 ± 0.02	3.3 ± 0.1	200°C 100°C 25°C

(a) is TiO_2(H_2 pre)

(a^*) is TiO_2(H_2 pre) treated using photoreduction conditions but without adding H_2PtCl_6.

Table 2. Surface composition and XPS Binding Energies.

No	Sample	Treatment	BE/eV Ti(2p3/2)	Pt(4f7/2)	O(1s)	Surface Atomic Ratio Pt/Ti	O/Ti	C/Ti	Minor Surface Contaminant S	P	C
A	TiO_2(anatase)	Degassed at 25°C	459.0	----	529.7	0.00	3.12	1.53	Y(b)	Y	Y
B	Oxidized Pt/TiO (N_2 Prep)	Degassed at 25°C	458.9 (1.83)(d)	71.1 (1.85)	530.0	0.11	3.60	1.29	N	N	N
C	Oxidized(c) Pt/TiO (N_2 Prep)	Degassed and 200°C Reduced at 500°C Degassed at 450°C	458.3 (1.44)	70.7 (2.00)	529.8	0.07	3.02	0.5	Y	N	N
D	Pt/TiO(a) (N_2 Prep) photo plastinized	Degassed at 25°C	458.4	70.4	529.6	0.13	5.75	5.9	Y	N	N
E	Pt/TiO (N_2 Prep) photo plastinized	Degassed at 200°C Reduced at 200 Degassed at 200°C	458.5 (1.93)	70.5	529.8	0.06	3.47	2.30	N	N	N
F	Pt/Ti_2O_3	Degassed at 200°C Reduced at 200°C Degassed at 200°C	458.9 (1.67)	70.9 (1.95)	530.2	0.20	3.44	1.46	N	N	Y
G	Pt/Ti_2O_3	Degassed at 200°C Reduced at 500°C Degassed at 450°C	458.6 (1.55)	71.0 (2.09)	530.0	0.15	3.20	1.44	N	N	Y
H*	Pt/TiO	Degassed at 200°C Reduced at 200°C Degassed at 200°C	458.0 (1.67)	70.5 (1.95)	529.8	0.36	3.02	2.28	Y	N	Y
I	Pt/Al_2O_3	Degassed at 25°C				C/O = 0.48			Y	N	Y
J*	Pt/Ti_4O_7 (SMSI)	Degassed at 25°C Overnight				0.31	3.42	0.48	N	Y	Y
K*	Pt/TiO (SMSI)	Degassed at 25°C Overnight				0.11	2.00	0.18	Y	N	Y

(a)The pellet was prepared with paraffin paper as described in the text.

(b) Y = Detectable, N = Not detectable.

(c) * = SMSI property (strongly reduced H_2 chemisorption) is known to be present for this material.

(d) Full width at half maximum in eV.

Table 4.

The correlation of SMSI behavior with electronic properties of supports.

Support Material	Carrier Type	Electrical Conductivity $ohm^{-1}cm^{-1}$	SMSI	Reference
TiO	Metal	10^{-1}	Y	a
Ti_2O_3	n	10^{-3}	Y	a
TiO_2	n	10^{-11}	N	a
Nb_2O_5	n	10^{-1}(200°C)	Y	17
V_2O_3	Metal	10^{+3}	Y	17, 31
HfO_2	p	10^{-5}(400°C)	N	17, 31
ZrO_2	p	10^{-5}(400°C)	N	17
Sc_2O_3	p	10^{-7}(650°C)	N	17, 31
MgO	n	10^{-12}	N	17, 31
SiO_2	Insul[b]	10^{-12}	N	17, 31
Al_2O_3	Insul	10^{-12}	N	17, 31
SiC	Metal	10^{-3}	Y	19

(a) This paper.

(b) Insulator

FIGURE CAPTIONS

Figure 1. H_2 uptake curves for platinized titanium oxides. (a) oxidized $Pt/TiO_2(H_2$ pre), ■, (b) $Pt/TiO_2(H_2$ pre), □, (c) Pt/Ti_2O_3, ▲, (d) Pt/TiO, ●.

Figure 2. H_2 uptake curves for titanium oxides. ■, TiO_2; □, $TiO_2(H_2$ pre); ▲, Ti_2O_3.

Insert is H_2 uptake curve for 5% Pt/Al_2O_3 and the axes plot the same variables as the larger figure.

Figure 3. Ti(2p) XPS spectra for some of the systems listed in Table 2. (B) Oxidized $Pt/TiO_2(H_2$ pre). (F) Pt/Ti_2O_3, H_2 reduction at 200°C. (C) Oxidized $Pt/TiO_2(H_2$ pre), reduced in-situ at 500°C. (H) Pt/TiO, H_2 reduction at 200°C. (G) Pt/Ti_2O_3, H_2 reduction at 500°C.

Figure 4. Pt(4f) XPS spectra for some of the systems of Table 2. (B) Oxidized $Pt/TiO_2(H_2$ pre), 50 eV pass energy. (E) $Pt/TiO_2(H_2$ pre), H_2 reduction at 200°C, 50 eV pass energy. (F) Pt/Ti_2O_3, H_2 reduction at 200°C, 25 eV pass energy. (H) Pt/TiO, H_2 reduction at 200°C, 25 eV pass energy.

Figure 5. Schematic reaction profiles for H_2 interacting with Pt/TiO_2 systems without, (a), and with, (b), the SMSI property.

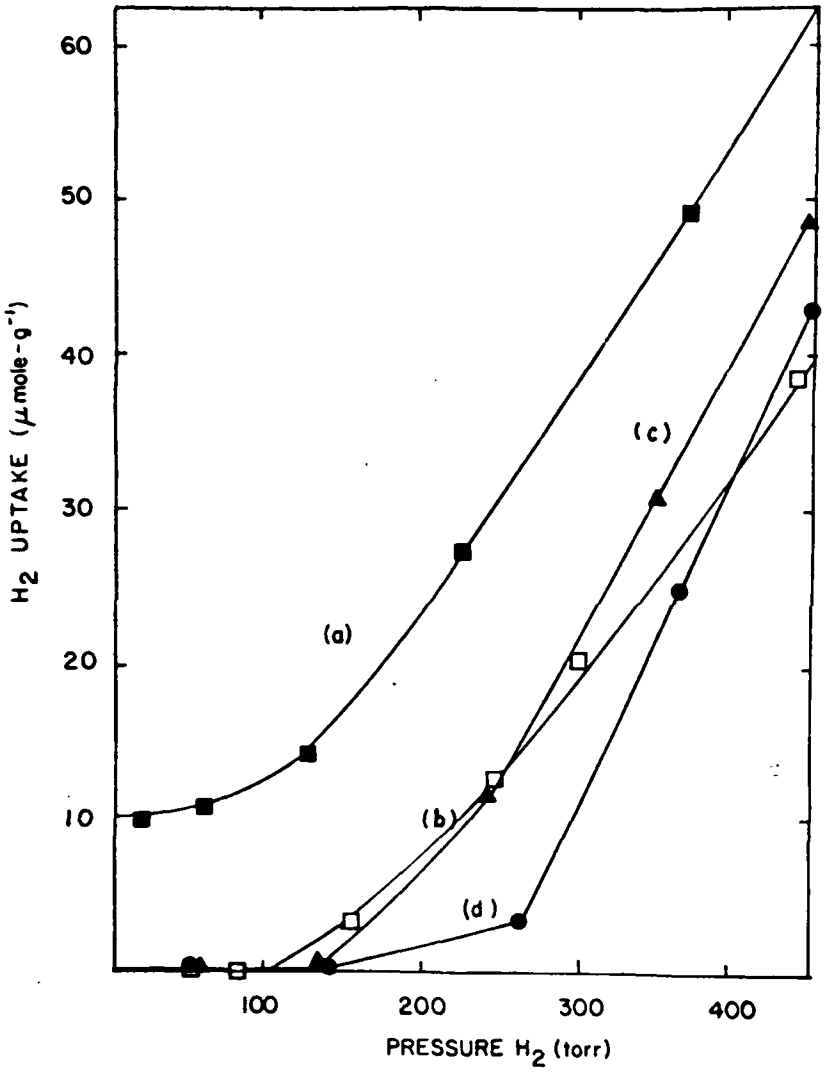

Chem, Lett. ; Fig 1

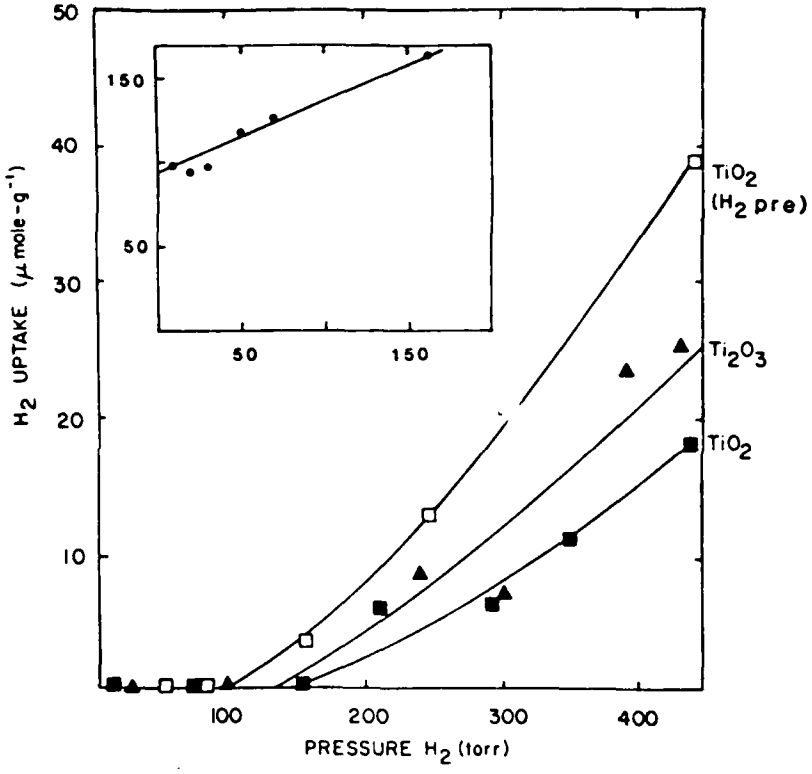

Chem, Lett : Fig. 2.

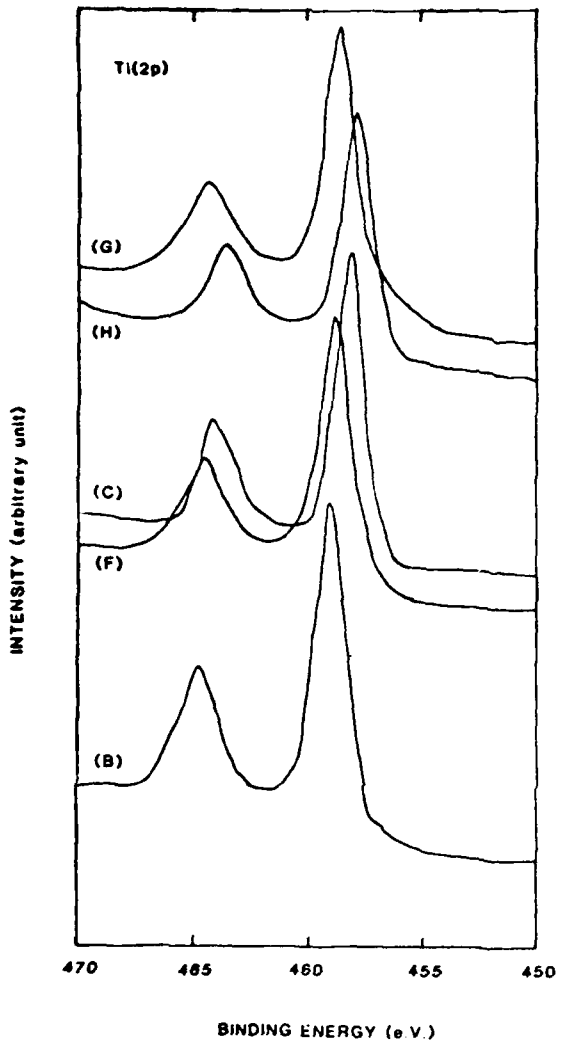

Chem, Whits : Fig 3

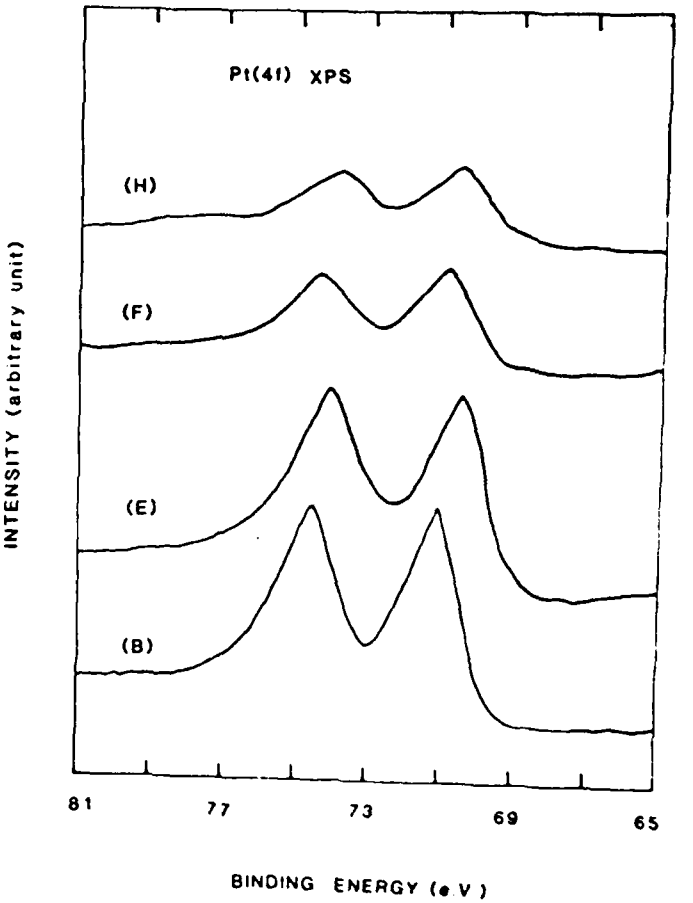

Chem, Whits : Fig 4

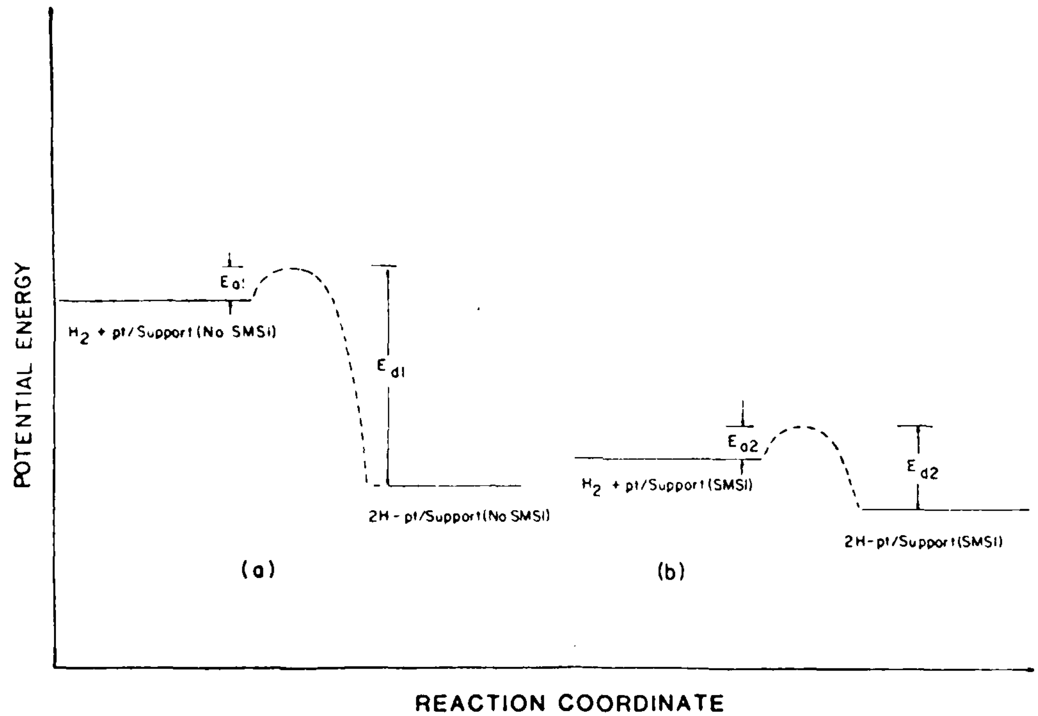

Chen, White : Fig 5

TECHNICAL REPORT DISTRIBUTION LIST, 056

	No. Copies
Dr. S. Sibener Department of Chemistry James Franck Institute 5640 Ellis Avenue Chicago, Illinois 60637	1
Dr. M. G. Lagally Department of Metallurgical and Mining Engineering University of Wisconsin Madison, Wisconsin 53706	1
Dr. Robert Gomer Department of Chemistry James Franck Institute 5640 Ellis Avenue Chicago, Illinois 60637	1
Dr. P. D. Kaplan Department of Physics University of California, Irvine Irvine, California 92664	1
Dr. D. Ramaker Chemistry Department George Washington University Washington, D.C. 20052	1
Dr. P. Hansma Chemistry Department University of California, Santa Barbara Santa Barbara, California 93106	1
Dr. P. Hansma Physics Department Stanford University Stanford, California	1
Professor R. Hall Chemistry Department Lehigh University Bethlehem, Pennsylvania 18502	1
Dr. J. C. Hemminger Chemistry Department University of California, Irvine Irvine, California 92717	1

	No. Copies
Dr. Martin Fleischmann Department of Chemistry Southampton University Southampton SO9 5NH Hampshire, England	1
Dr. J. Osteryoung Chemistry Department State University of New York at Buffalo Buffalo, New York 14214	1
Dr. G. Rubloff I.B.M. Thomas J. Watson Research Center P. O. Box 218 Yorktown Heights, New York 10598	1
Dr. J. A. Gardner Department of Physics Oregon State University Corvallis, Oregon 97331	1
Dr. B. D. Dunn Materials Engineering Department Northwestern University Evanston, Illinois 60201	1
Dr. K. D. Gillis Chemistry Department Northwestern University Evanston, Illinois 60201	1
Dr. R. W. Plummer University of Pennsylvania Department of Physics Philadelphia, Pennsylvania 19104	1
Dr. E. Yeager Department of Chemistry Case Western Reserve University Cleveland, Ohio 44106	2
Professor D. Landolt University of Pittsburgh Chemistry Department Pittsburgh, Pennsylvania 15260	1

	No. Copies
[illegible]	1
[illegible]	1
[illegible]	1
[illegible]	1
[illegible]	1
[illegible]	1
Dr. A. G. Baston Hughes Research Laboratories 3011 Malibu Canyon Road Malibu, California 90265	1
Dr. Stephen Webber Dept. of Chemistry University of Texas Austin, TX 78712	1
Dr. A. J. Bard Dept. of Chemistry University of Texas Austin, TX 78712	1

TECHNICAL REPORT DISTRIBUTION LIST, GEN

	No. Copies
Office of Naval Research Attn: Code 472 800 North Quincy Street Arlington, Virginia 22217	2
ONR Western Regional Office Attn: Dr. R. J. Marcus 1030 East Green Street Pasadena, California 91106	1
ONR Eastern Regional Office Attn: Dr. L. H. Peebles Building 114, Section D 666 Summer Street Boston, Massachusetts 02210	1
Director, Naval Research Laboratory Attn: Code 6100 Washington, D.C. 20390	1
The Assistant Secretary of the Navy (RE&S) Department of the Navy Room 4E736, Pentagon Washington, D.C. 20350	1
Commander, Naval Air Systems Command Attn: Code 310C (H. Rosenwasser) Department of the Navy Washington, D.C. 20360	1
Defense Technical Information Center Building 5, Cameron Station Alexandria, Virginia 22314	12
Dr. Fred Saalfeld Chemistry Division, Code 6100 Naval Research Laboratory Washington, D.C. 20375	1
Mr. James Kelley DTNSRDC Code 2803 Annapolis, Maryland 21402	1
Mr. A. M. Anzalone Administrative Librarian PLASTEC/ARRADCOM Bldg 3401 Dover, New Jersey 07801	1
U.S. Army Research Office Attn: CRD-AA-IP P.O. Box 1211 Research Triangle Park, N.C. 27709	1
Naval Ocean Systems Center Attn: Mr. Joe McCartney San Diego, California 92152	1
Naval Weapons Center Attn: Dr. A. B. Amster, Chemistry Division China Lake, California 93555	1
Naval Civil Engineering Laboratory Attn: Dr. R. W. Drisko Port Hueneme, California 93401	1
Department of Physics & Chemistry Naval Postgraduate School Monterey, California 93940	1
Scientific Advisor Commandant of the Marine Corps (Code RD-1) Washington, D.C. 20380	1
Naval Ship Research and Development Center Attn: Dr. G. Bosmajian, Applied Chemistry Division Annapolis, Maryland 21401	1
Naval Ocean Systems Center Attn: Dr. S. Yamamoto, Marine Sciences Division San Diego, California 91232	1
Mr. John Boyle Materials Branch Naval Ship Engineering Center Philadelphia, Pennsylvania 19112	1

TECHNICAL REPORT DISTRIBUTION LIST, 056

	No. Copies
Dr. G. A. Somorjai Department of Chemistry University of California Berkeley, California 94720	1
Dr. L. N. Jarvis Surface Chemistry Division 4555 Overlook Avenue, S.W. Washington, D.C. 20375	1
Dr. J. B. Hudson Materials Division Rensselaer Polytechnic Institute Troy, New York 12181	1
Dr. John T. Yates Surface Chemistry Section National Bureau of Standards Department of Commerce Washington, D.C. 20234	1
Dr. Theodore E. Madey Surface Chemistry Section Department of Commerce National Bureau of Standards Washington, D.C. 20234	1
Dr. J. M. White Department of Chemistry University of Texas Austin, Texas 78712	1
Dr. Keith H. Johnson Department of Metallurgy and Materials Science Massachusetts Institute of Technology Cambridge, Massachusetts 02139	1
Dr. J. E. Demuth IBM Corporation Thomas J. Watson Research Center P.O. Box 218 Yorktown Heights, New York 10598	1
Dr. C. P. Flynn Department of Physics University of Illinois Urbana, Illinois 61801	1
Dr. W. Kohn Department of Physics University of California (San Diego) LaJolla, California 92037	1
Dr. R. L. Park Director, Center of Materials Research University of Maryland College Park, Maryland 20742	1
Dr. W. T. Peria Electrical Engineering Department University of Minnesota Minneapolis, Minnesota 55455	1
Dr. Chia-wei Woo Department of Physics Northwestern University Evanston, Illinois 60201	1
Dr. D. C. Mattis Polytechnic Institute of New York 333 Jay Street Brooklyn, New York 11201	1
Dr. Robert M. Hexter Department of Chemistry University of Minnesota Minneapolis, Minnesota 55455	1
Dr. R. P. Van Duyne Chemistry Department Northwestern University Evanston, Illinois 60201	1

END

DATE
FILMED

8-82

DTIC